International Journal of Engineering Innovation & Research
Volume 10, Issue 2, ISSN: 2277 – 5668

Crown Structure Design of Radial Tire with Imitation Cat Claw Pad

Mengyu Xie[1], Lanian Tang[2], Yanhong Gao[2], Ruifeng Sun[3], Congzhen Liu[1*] and Chengwei Xu[1]
[1] School of Transportation and Vehicle Engineering, Shandong University of Technology, Shandong, Zibo, Zhangdian, 255049, China.
[2] Shandong Tangjun Ouling Automobile Manufacture Co., Ltd. Shandong, Zibo, Zichuan, 255000, China.
[3] Forestry College, Shandong Agricultural University, Shandong, Taian, Taishan, 271018, China.
*Corresponding author email id: lcz200811@163.com

Date of publication (dd/mm/yyyy): 08/04/2021

***Abstract* – In order to alleviate the inherent contradiction between tire grip and wear performance, a 205/55R16 passenger car radial tire was taken as the research object, the bionic design of tire crown was carried out. The dynamic grounding characteristics of cat front PAWS were obtained by Walkway pressure testing system, and the reverse topology was carried out with 3D laser scanner. The point cloud of the cross section of cat paw pad was fitted by polynomial fitting. The bionic design of the tire crown was carried out based on the similarity principle. ABAQUS model was established to compare the grounding area and pressure distribution of the bionic tire and the sample tire under the tilting and deflection condition under static load. The results show that the bionic tire design can effectively increase the ground area, reduce the peak ground pressure, improve the tire eccentric wear phenomenon, and realize the synergistic improvement of tire grip and wear performance.**

***Keywords* – The Bionic Tire, Tyre Crown, The Grounding Performance, Finite Element Analysis.**

I. INTRODUCTION

As a part of wheeled vehicles that directly contact with the ground, the performance of the tire has an important impact on the vehicle handling stability, safety, comfort, economy and so on. The tire crown is the only contact part between the tire and the ground, which determines the tire's grounding performance. Y. Tanaka et al. [1] explored the influence on wear performance by changing the connection mode of fetal crown arc. Liang Chen [2] proposed the evaluation index of tire ground catching performance and explained the influencing factors of tire ground catching performance by studying tire comprehensive ground performance. Peng Xudong et al. [3] found that the temperature had a certain influence on the tread compound modulus, and then had a significant influence on the tire grip. Cho J.R. et al. [4] used numerical analysis method of wear model to optimize tread pattern and improve tire wear performance. However, there is inherent contradiction between tire grip and wear performance, and it is mutually restricted with rolling resistance, forming devil triangle relationship [5].

In recent years, with the development of biological science and technology, bionics combined with basic disciplines has made great progress in mechanical bionics, medical bionics, electronic bionics, etc. [6-8]. In the field of tire design, German Continental [9] designed the imitation leopard paw tire through bionics, which can increase the tire-road contact area and reduce the braking distance when the vehicle is braking. Zhou Likun et al. [10] took octopus suckers as bionic objects and designed bionic sucker tires to improve the braking performance of vehicles on ice. Li Jie et al. [11] studied the static and dynamic characteristics of desert bionic tire by using experimental and theoretical analysis methods. Cong Qian et al. [12] numerically simulated the flow fields on three different bionic non-smooth grooves, and analyzed the influence of grooves shape on drag reduction effect. Wang Guolin et al. [13] designed the tire crown structure by imitating locust feet, and improved the grip and

International Journal of Engineering Innovation & Research
Volume 10, Issue 2, ISSN: 2277 – 5668

wear performance of the tire. Fan Shasha et al. [14] transplanted the bionic pit non-smooth structure into the design of tire pattern groove wall. Through noise and sound pressure comparison, the bionic structure can reduce the generation of pattern noise. The research status at home and abroad shows that bionics has made many important achievements in tire design and application, and has gradually become a new way to optimize tire performance.

This article uses the WALKWAY pressure test system with 3D laser scanner for the cat paw grounding characteristics are studied, using the similar principle of cat's paw palm pad arc curve fit is used in the design of the passenger car tire crown, explore the tire cornering condition static load swaying grounding area and pressure distribution situation, in order to achieve the performance of two synergy ascension.

II. Fetal Crown Structure Design of Imitation Cat Claw Palm Pad

The dynamic grounding characteristics of cat claws were obtained by the joint testing of Olympus high-speed camera and Walkway pressure testing system. The test bed layout is shown in Figure 1. Pressure sensor 2 was placed on the surface of runway 5 and connected to the computer through data transmission line 3. Healthy adult cats were selected to pass the test, the cat is lured to walk between the transparent baffles 4 by means of food and light spots [15], walkway pressure test system was used to collect the grounding motion data when the cat claws passed, and Olympus high-speed camera 1 was used for shooting.

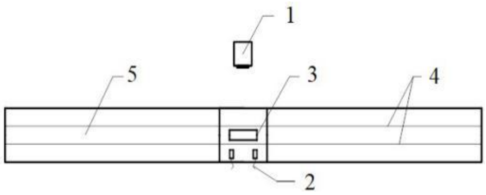

Fig. 1. Schematic diagram of test bed.

When cats are moving, their front paws mainly play the role of support and direction control [16], so as to ensure sufficient lateral force during steering. The front PAWS of cats were selected as the research object, and the research variable was forward speed. The vertical reaction force of cat claw pad and each claw toe was extracted, and the change curve of grounding pressure at each position was drawn (for example, the speed was 1.34m/s), as shown in Figure 2.

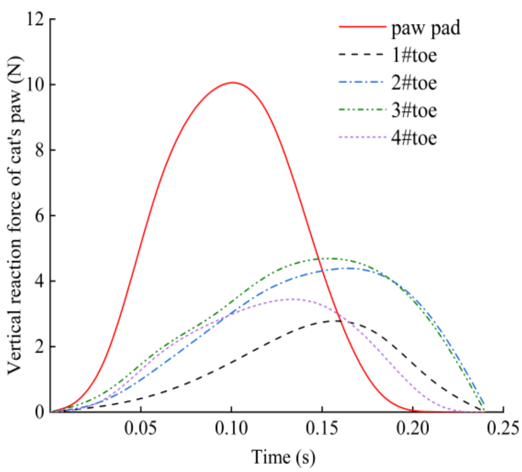

Fig. 2. The reaction curve of each part of cat's front paw.

As can be seen from Figure 2, in the process of stable contact between the cat's front paw and the ground, the palm pad is always the part with the largest force. At other velocities, the variation trend of the ground reaction at all positions is consistent, indicating that the palm pad is the main supporting position when the cat paw is grounded. With this as the inspiration, the shape characteristics of cat paw pad were extracted and applied to the design of tire crown arc of passenger car.

A 3D laser scanner of Vivid 910 was used to scan the paw pad of the cat's front paw, and the accurate geometric profile of the cat's paw was obtained. The geometrical shape diagram was simplified using Image ware, as shown in Fig. 3. Cross section points were intercepted for curve fitting to obtain the cross section curve of the paw pad of the cat's front paw, as shown in Fig. 4.

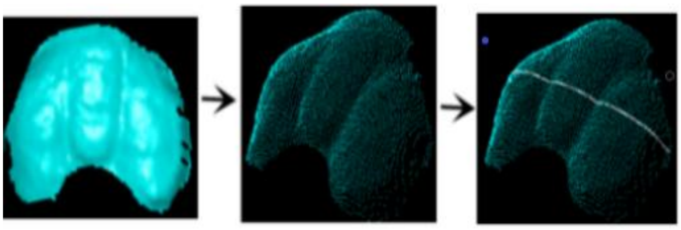

Fig. 3. Cat claw point cloud processing process.

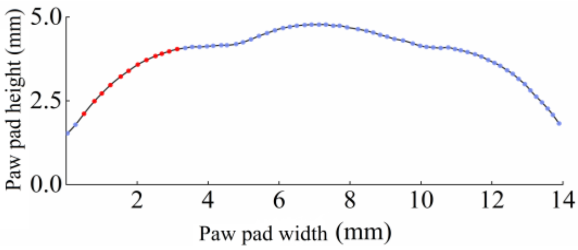

Fig. 4. Cat paw pad point cloud cross-section fitting curve.

On the basis of the point cloud at the shoulder of the palm cushion section (Fig. 4 red curve), polynomial fitting was performed, where the fitting equation was:

$$y = 1.4439 + 1.5510x - 0.2709x^2 + 0.0131x^3 \qquad (1)$$

According to the similarity principle [17], the bionic design of tire crown arc is carried out with equation (1) as the prototype, as shown in Fig. 5. The bionic tire crown arc is shown as the red mark in the figure.

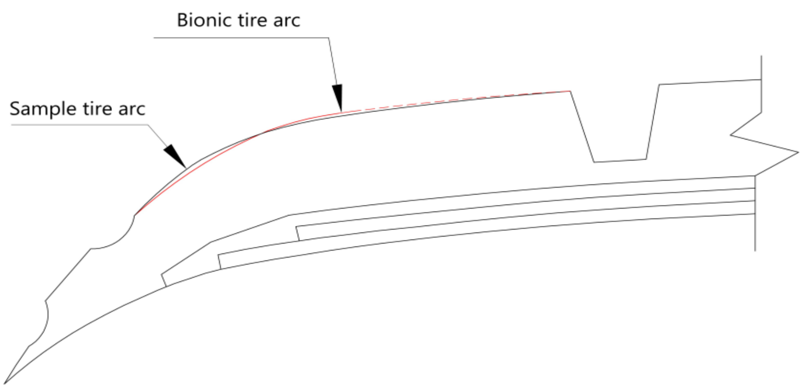

Fig. 5. 205/55 R16 tire crown arc.

III. Establishment and Verification of Tire Model

A. *Finite Element Model*

Due to the complexity of tire structure and the non-linearity of rubber materials, each component is characterized by different materials [18]. The body and the belt layer are rubber-cord composite materials, which are simulated by the REBAR material model. The properties of the material model are shown in Table 1. The Yeoh material model is used to simulate rubber materials such as tread and body, and the strain energy constitutive equation of the Yeoh model is [19]:

$$W = C_{10}(I_1 - 3) + C_{20}(I_1 - 3)^2 + C_{30}(I_1 - 3)^3 \tag{2}$$

Where W is the strain energy; C_{10}, C_{20} and C_{30} are the expansion coefficients of the third-order reduced polynomial; I_1 is the first invariant of strain.

Table 1. Reinforcement material properties.

Rebar Material	Young's Modulus(MPa)	Poisson's Ratio (μ)	Density (kg/m³)	Cord Angle (°)
Belt steel wire 1	105900	0.29	7800	66
Belt steel wire 2	105900	0.29	7800	114
Carcass cords	5250	0.3	1350	0

B. *Model Verification*

In order to verify the accuracy and applicability of the tire finite element model, the CSS-88100 static loading testing machine was used to conduct loading tests on the tire under test, and the load and grounding marks were measured, as shown in Fig. 6. The maximum rated load of the tire is 6150N, and the charging pressure is 2.6bar when loading. Under static loading, the test and simulation results of load-subsidence are shown in Fig. 7. The relationship between load and subsidence is approximately linear and the error is within a small range.

Fig. 6. Static loading test.

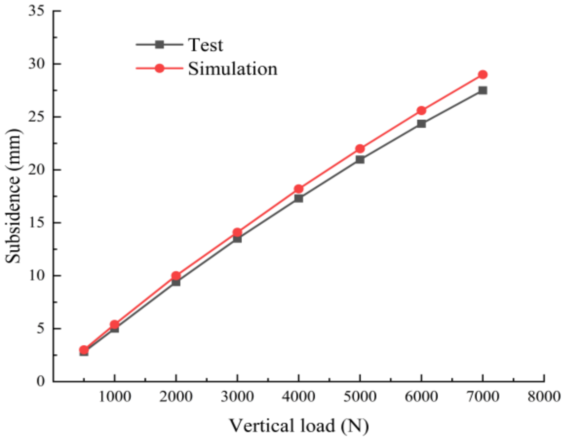

Fig. 7. Load - subsidence curve.

The shape comparison of ground mark of tire under static load is shown in Fig. 8. The mark distribution of test and simulation is in good agreement. Numerical comparison between the test and simulation is shown in Table 2. The maximum error between the test and simulation is 3.8%, indicating high precision. Therefore, the tire model can be used for the next simulation analysis.

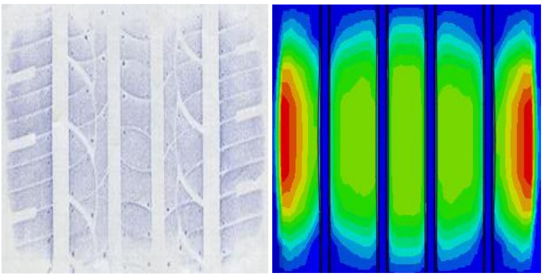

Fig. 8. Contact patch shape under static load.

Table 2. Comparison of contact patch test and simulation results.

Project	Test	Simulation	Relative error /%
Long axis length of contact patch /mm	150.32	147.19	2.1
short axis length of contact patch /mm	115.93	113.16	2.4
Grounding area /mm^2	15631	15039	3.8

IV. Results Analysis and Discussion

A. *Static Load Grounding Performance Analysis*

Through static loading analysis, the ground pressure distribution between the sample tire and the bionic tire is obtained, as shown in Figure 9. It can be seen from the figure that after bionic design of the fetal crown arc, the rectangular rate of the earthing trace of the fetal crown is improved. The ground pressure in the tread center increased, and the peak pressure in the shoulder stress concentration area decreased, and the ground mark in the high stress area of the shoulder changed from shuttle to trapezoid. Under the premise of maintaining stable ground area, the peak ground pressure of sample tire and bionic tire is 0.54MPa and 0.47MPa respectively, the peak ground pressure is reduced by 13%, and the pressure distribution is more uniform. The results show that the bionic structure design can ensure the tire's stable ground condition under static load.

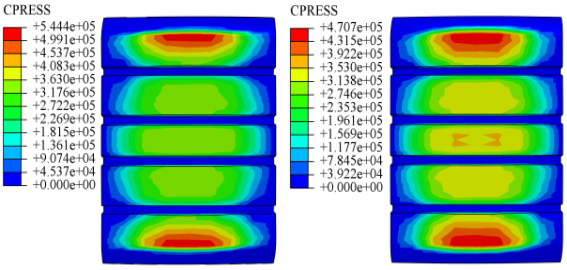

(a) Sample tire. (b) Bionic tire.

Fig. 9. Ground pressure distribution of tire under static load

B. *Tilting Ground Performance Analysis*

Through the roll loading analysis, the ground pressure distribution of sample tire and bionic tire under different roll angles was obtained, as shown in Fig. 10.Table 3 shows the tilting ground data of tire under static load. It can be seen from Fig. 10 and Table 3 that the variation trend of ground marks of the sample tire and the bionic tire is similar, which decreases with the increase of the roll Angle. The length of the imprint increases on the ground side and decreases on the other side, gradually changing from trapezoid to triangle. Under different roll angles, the ground area of the bionic tire did not change significantly compared with the sample tire, but the peak ground pressure and the skewness of the ground pressure decreased significantly, the high ground pressure area of the shoulder increased, and the stress concentration area decreased. The results show that the bionic structure design can improve the uniform distribution of ground pressure and enhance the tire wear performance under tire roll condition.

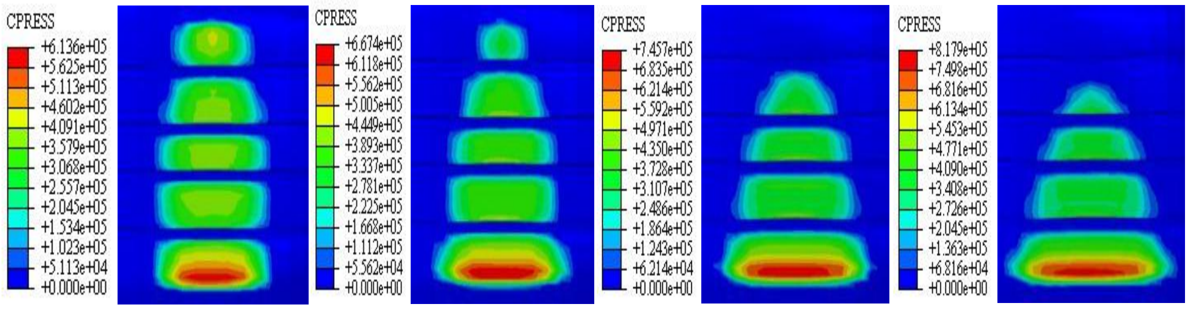

Tilt 2° Tilt 4° Tilt 6° Tilt 8°

(a) Sample tire.

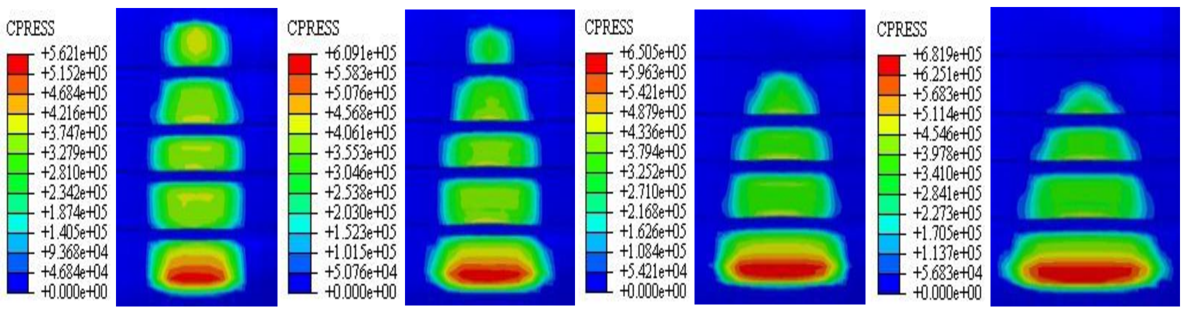

Tilt 2° Tilt 4° Tilt 6° Tilt 8°

(b) Bionic tire

Fig. 10. Distribution of static load ground pressure under different tilt angle.

Table 3. Tyre tilting ground data under static load.

Scheme	Peak Ground Pressure/MPa			Ground Pressure Deflection Value/MPa			Ground Contact Area/cm^2		
	Sample Tire	Bionic Tire	Difference Value	Sample Tire	Bionic Tire	Difference Value	Sample Tire	Bionic Tire	Difference Value
2°	0.6136	0.5621	-8.4%	0.1432	0.1356	-5.3%	141.91	142.75	0.59%
4°	0.6674	0.6091	-8.7%	0.1512	0.1395	-7.7%	137.97	139.75	1.29%
6°	0.7457	0.6505	-12.8%	0.1685	0.1536	-8.8%	130.81	133.21	1.83%
8°	0.8179	0.6819	-16.6%	0.1816	0.1648	-9.3%	128.31	130.47	0.89%

C. *Lateral Grounding Performance Analysis*

Tire sideshow has an important effect on vehicle handling stability. When side-deflection occurs, the shoulder of the tire is the main force area, and the simulation of different side-deflection angles is realized by the lateral and longitudinal decomposition of the tire speed. The lateral angles are 2, 4, 6, and 8. The tire side grounding pressure distribution and grounding parameters are obtained, as shown in Fig. 11 and Table 4.

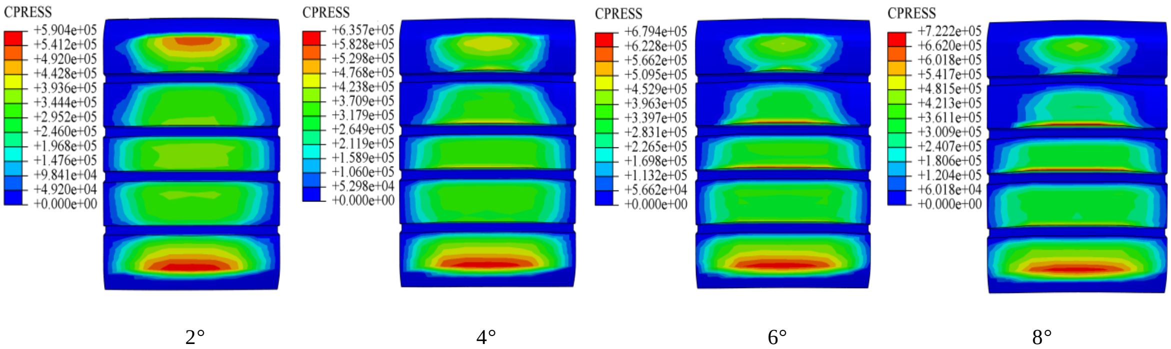

(a) Sample tire.

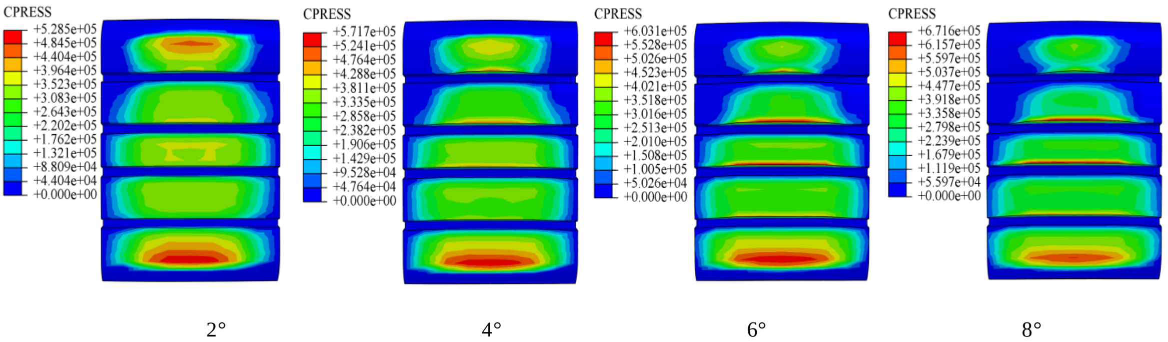

(b) Bionic tire.

Fig. 11. Tire ground pressure distribution under different lateral deviation angles.

Table 4. Tire lateral deviation ground data.

Scheme	Cornering force/N			Peak Ground Pressure/MPa			Ground Pressure Deflection Value/MPa			Ground Contact Area/cm^2		
	Sample Tire	Bionic Tire	Difference Value	Sample Tire	Bionic Tire	Difference Value	Sample Tire	Bionic Tire	Difference Value	Sample Tire	Bionic Tire	Difference Value
2°	626	631	0.8%	5.9035	5.2852	-10.5%	0.1272	0.1186	-6.8%	148.87	152.60	2.5%

Scheme	Cornering force/N			Peak Ground Pressure/MPa			Ground Pressure Deflection Value/MPa			Ground Contact Area/cm^2		
	Sample Tire	Bionic Tire	Difference Value	Sample Tire	Bionic Tire	Difference Value	Sample Tire	Bionic Tire	Difference Value	Sample Tire	Bionic Tire	Difference Value
4°	1190	1207	1.4%	6.3574	5.7169	-10.1%	0.1332	0.1284	-3.6%	139.20	143.34	3.0%
6°	1760	1791	1.8%	6.7939	6.0311	-11.2%	0.1604	0.1541	-3.9%	144.19	149.34	3.6%
8°	2086	2134	2.3%	7.2222	6.7162	-7.0%	0.1711	0.1666	-2.6%	141.27	149.58	5.9%

As can be seen from the chart, with the increase of the side Angle, the tire ground mark changes from rectangle to trapezoid, and the ground area shows a downward trend. The peak ground pressure gradually increases and transfers from the shoulder position to the edge of the rib pattern in the ground center, which results in the decrease of the uniform distribution of ground pressure on the tread and the serious deviant wear. Compared with the sample tire, the bionic tire's lateral force increased by 2.3% and the peak ground pressure decreased by 11.2, the standard deviation of grounding pressure decreased by 6.8% and the area of grounding increased by 5.9%. The bionic tire crown design can effectively increase the ground area of the tire, enhance the lateral grip, reduce the deviation wear, and improve the vehicle handling stability under the lateral deflection condition.

V. Conclusion

The structure characteristics of the cat claw were studied, and the geometric shape of the cat claw was obtained with a scanner. Based on the geometric shape of the cat paw pad, the crown structure of the 205/55R16 radial tire was designed. The finite element software was used to build the model and carry out simulation analysis, and the following conclusions were drawn:

1. Under the condition of static load, the peak ground pressure of the bionic tire is reduced by 13% and the pressure distribution is more uniform under the premise of maintaining a stable ground area. The results show that the bionic structure design can ensure the tire’s stable ground condition under static load.

2. Under the roll condition, the variations of the ground marks of the sample and bionic tire decreased with the increase of the roll Angle, and gradually changed from trapezoid to triangle. Compared with the sample tire, the peak grounding pressure and grounding pressure skewness of the bionic tire decreased obviously, and the stress concentration area of the shoulder decreased. The results show that the bionic structure design can improve the uniform distribution of ground pressure and enhance the wear performance of tire under roll static load condition.

3. In the lateral condition, with the increase of the lateral angle, the ground imprint changes from rectangle to trapezoid, the peak pressure increases and the ground area decreases gradually. Compared with the sample tire, the bionic tire can effectively enhance the lateral grip, relieve the stress concentration, and improve the vehicle handling stability.

References

[1] Tanaka Y, Ohishi K. Unified approach to optimization of tread pattern shape and cross-sectional contour of tires [J]. Tire Science and Technology, 2010, 38(4): 276-285.

[2] Chen Liang. Research on the comprehensive grounding performance evaluation system and method of radial tire [D]. Zhenjiang: Jiangsu University, 2013.

[3] Xu-dong Peng. The friction between rubber and tires [J]. Rubber Industry, 2003(09): 562-568.
[4] Cho J.R., Choi J.H., Kim Y.S. Abrasive wear amount estimate for 3D patterned tire utilizing frictional dynamic rolling analysis [J]. Tribology International, 2011, 44(7): 850-858.
[5] Yuan Tang. Research progress on performance balance of high performance tire tread rubber magic triangle [J]. Rubber Industry, 2019, 66(05): 388-394.
[6] Lan Lan, Yan Fang, Ding-qiJi. Progress and prospect of bionics applications [J]. Science and technology communication, 2019, 11(22): 149-150 + 153.
[7] Jian Ye, Xin-ying Huang. Design and construction technology of calla lily flower bionic energy-saving building [J]. Construction Science and technology, 2019(11): 70-76.
[8] Yuan He. Research on energy saving and vibration abatement mechanical leg imitating ostrich rear limb [D]. Jilin University, 2018.
[9] Lu Xu, Li-kunZhou. Research status and prospects of bionic tire [J]. Rubber Industry, 2018, 65(01): 113-115.
[10] Li-kunZhou, Hong-wei Wang. Tread pattern design and finite element analysis of copycat fish sucker [J]. Journal of xi 'an university of technology, 2013, 29(2): 228-231.
[11] Jie Li, Ji-de Zhuang, Dong Wei. Design and experimental study of imitation camel's foot rubber used in desert [J]. Journal of agricultural engineering, 1999, 15(2): 32-36.
[12] Cong Qian. Influence of bionic non-smooth groove shape on drag reduction effect [J]. Journal of Hydrodynamics Research and Progress (Series A), 2006 (02): 232-238.
[13] Guo-LinWang, Yin-Wei Ma, ChenLing, et al. Structure design of radial tire crown imitating locust foot [J]. Journal of mechanical engineering, 2013, 49(12): 131-135.
[14] Sha-sha Fan, Hai-chao Zhou. Noise reduction analysis of bionic tire pattern with Pit [J]. Science and technology innovation herald, 2015, 12(21): 60-61+64.
[15] Alexander R.M.N., Jayes A.S. A dynamic similarity hypothesis for the gaits of quadrupedal mammals [J]. J. Zool., Lond, 1983(201): 135-152.
[16] Ya-zhongLiu. Research on gait planning and control method of crawling motion of feline quadruped Robot [D]. Harbin university of Science and Technology, 2018.
[17] Huan-huanZuo. Application exploration of similarity principle [J]. Industry and technology forum, 2016, 15(20): 73.
[18] Yao Zhen. Tire ground behavior analysis based on ABAQUS modeling [D]. Ningbo: Ningbo University, 2015.
[19] JunWang, Liang Li, LinSun. Finite element analysis of 245/70R16 tires [J]. Tire Industry. 2016, (9): 520-528.

AUTHOR'S PROFILE

First Author
Mengyu Xie, Master in reading, Male, School of Transportation and Vehicle Engineering, Shandong University of Technology, Shandong, Zibo, Zhangdian, 255049, China. email id: 328097596@qq.com

Second Author
Lanian Tong, Bachelor, Male, Shandong Tangjun Ouling Automobile Manufacture Co., Ltd, Shandong, Zibo, Zichuan, 255000, China.

Third Author
Yanhong Gao, Bachelor, Female, Shandong Tangjun Ouling Automobile Manufacture Co., Ltd, Shandong, Zibo, Zichuan, 255000, China.

Fourth Author
Ruifeng Sun, Bachelor in reading, Female, Shandong Agricultural University, Shandong, Taian, Taishan, 271018, China.

Fifth Author
Congzhen Liu, Doctor of Engineering (Correspondence author), Male, Associate Professor, School of Transportation and Vehicle Engineering, Shandong University of Technology, Shandong, Zibo, Zhangdian, 255049, China.

Sixth Author
Chengwei Xu, Master in reading, Male, School of Transportation and Vehicle Engineering, Shandong University of Technology, Shandong, Zibo, Zhangdian, 255049, China.